Tunable complex stability in surface molecular recognition mediated by self-complementary quadruple hydrogen bonds

Zou, Shan; Zhang, Zhihong; Förch, Renate; Knoll, Wolfgang; Schönherr, Holger; Vancso, G. Julius

National Research Council Canada   Conseil national de recherches Canada

Canada

Tunable Complex Stability in Surface Molecular Recognition Mediated by Self-Complementary Quadruple Hydrogen Bonds

Shan Zou,[†] Zhihong Zhang,[‡] Renate Förch,[‡] Wolfgang Knoll,[‡]
Holger Schönherr,[†] and G. Julius Vancso*,[†]

Materials Science and Technology of Polymers, MESA+ Institute of Nanotechnology and Faculty of Science and Technology, University of Twente, 7500 AE Enschede, The Netherlands, and Max-Planck-Institute for Polymer Research, Ackermannweg 10, 55128 Mainz, Germany

We show that surfaces modified with asymmetric 2-ureido-4[1H]-pyrimidinone-hydroxyalkane disulfide adsorbates exhibit efficient and controllable self-complementary molecular recognition of the pyrimidinone moieties. Two novel asymmetric 2-ureido-4[1H]-pyrimidinone-hydroxyalkane disulfide adsorbates, as well as two trifluoromethyl- and ferrocenyl-derivatized external pyrimidinone guests, were synthesized. Self-complementary molecular recognition of the pyrimidinone moieties, mediated by a quadruple donor−donor−acceptor−acceptor array of hydrogen-bonding sites, was studied in self-assembled monolayers on Au by exploiting the dependence of the dimerization constant on the solvent and temperature. Depending on the choice of solvent and temperature, reversible supramolecular recognition between surface-immobilized adsorbates and external guests occurred, as shown by X-ray photoelectron spectroscopy, differential pulse voltammetry, atomic force microscopy, and surface plasmon resonance methods. We observe a surface-enhanced apparent dimerization constant, which depends on the solvent and temperature. This feature allows us to conveniently control the complex stability, which renders these systems highly suitable for the construction of more complex, directionally defined surface-immobilized supramolecular architectures, as well as for the study of pyrimidinone-based supramolecular polymers at surfaces.

Introduction

Self-organization in biological systems frequently relies on the utilization of multiple noncovalent interactions to define structure *and* achieve functionality.[1] Chief among the guiding principles is molecular recognition.[1−3] Based on the fundamental idea of exploiting weak, yet directional, multivalent interactions, biology-inspired supramolecular architectures[4] at surfaces do not only enhance the possibilities for fundamental studies[5] but can also be exploited in, for instance, (bio)sensor designs[6] or supramolecular assemblies at surfaces.[2,7] For example, Credo et al.[2f] demonstrated how exchange reactions of multiple hydrogen-bonded assemblies at self-assembled monolayers (SAMs) can be utilized to manipulate conductance in mesoscale structures. Current challenges include the increase of the complexity of the assemblies and the enhanced control of stability versus reversibility.[8]

High dimerization constants of the recognition units are a prerequisite for the formation of defined, robust complexes or supramolecular polymers, as shown by many authors.[9−11] For instance, large dimerization constants have been reported for 2-ureido-4[1H]-pyrimidinones ($>10^7$ M^{-1} in CDCl$_3$).[10,12] In recent years, there have been numerous reports on similarly strong dimerization of a variety of hydrogen-bonding systems.[13−16] The self-complementary molecular recognition of the previously mentioned pyrimidinone moieties, which is mediated by a quadruple donor−donor−acceptor−acceptor array of hydrogen-bonding sites, varies with the solvent composition and temperature [K in 15% dimethylsulfoxide (DMSO) in CDCl$_3$ = 51 M^{-1}; K decreases 10 times when T increases

* Corresponding author. E-mail: g.j.vancso@utwente.nl.
† University of Twente.
‡ Max-Planck-Institute for Polymer Research.

(1) (a) Buckingham, A. D.; Legon, A. C.; Roberts, S. M. *Principles of Molecular Recognition*; Blackie: London, 1993. (b) *The Lock and Key Principle: The State of the Art*; Behr, J.-P., Ed.; Wiley: Chichester, 1994.

(2) (a) Cooke, G.; Rotello, V. M. *Chem. Soc. Rev.* **2002**, *31*, 275−286. (b) Lehn, J. M. *Science* **2002**, *295*, 2400−2403. (c) Reinhoudt, D. N.; Crego-Calama, M. *Science* **2002**, *295*, 2403−2406. (d) Ikkala, O.; ten Brinke, G. *Science* **2002**, *295*, 2407−2409. (e) Whitesides, G. M.; Grzybowski, B. *Science* **2002**, *295*, 2418−2421. (f) Credo, G. M.; Boal, A. K.; Das, K.; Galow, T. H.; Rotello, V. M.; Feldheim, D. L.; Gorman, C. B. *J. Am. Chem. Soc.* **2002**, *124*, 9036−9037.

(3) (a) Motesharei, K.; Myles, D. C. *J. Am. Chem. Soc.* **1994**, *116*, 7413−7414. (b) Dawson, S. L.; Elman, J.; Margevich, D. E.; McKenna, W.; Tirrell, D. A.; Ulman, A. *ACS Symp. Ser.* **1996**, *627*, 187−196.

(4) (a) Lehn, J.-M. *Angew. Chem., Int. Ed. Engl.* **1988**, *27*, 89−112. (b) Cram, D. J. *Angew. Chem., Int. Ed. Engl.* **1988**, *27*, 1009−1020. (c) Pedersen, C. J. *Angew. Chem., Int. Ed. Engl.* **1988**, *27*, 1021−1027.

(5) See, for example: Schönherr, H.; Paraschiv, V.; Zapotoczny, S.; Crego-Calama, M.; Timmerman, P.; Frank, C. W.; Vancso, G. J.; Reinhoudt, D. N. *Proc. Natl. Acad. Sci. U.S.A.* **2002**, *99*, 5024−5027 and references therein.

(6) Häussling, L.; Ringsdorf, H.; Schmitt, F. J.; Knoll, W. *Langmuir* **1991**, *7*, 1837−1840.

(7) See, for example: García-López, J. J.; Zapotoczny, S.; Timmerman, P.; van Veggel, F. C. J. M.; Vancso, G. J.; Crego-Calama, M.; Reinhoudt, D. N. *J. Chem. Soc., Chem. Commun.* **2003**, 352−353.

(8) For a recent collection of articles regarding current challenges, see: Halpern, J. *Proc. Natl. Acad. Sci. U.S.A.* **2002**, *99*, 4762−4762 and following articles.

(9) Lehn, J.-M. *Macromol. Chem. Macromol. Symp.* **1993**, *69*, 1−17.

(10) Sijbesma, R. P.; Beijer, F. H.; Brunsveld, L.; Folmer, B. J. B.; Hirschberg, J. H. K. K.; Lange, R. F. M.; Lowe, J. K. L.; Meijer, E. W. *Science* **1997**, *278*, 1601−1604.

(11) For a recent review, see: Brunsveld, L.; Folmer, B. J. B.; Meijer, E. W.; Sijbesma, R. P. *Chem. Rev.* **2001**, *101*, 4071−4098.

(12) (a) Beijer, F. H.; Kooijman, H.; Spek, A. L.; Sijbesma, R. P.; Meijer, E. W. *Angew. Chem., Int. Ed. Engl.* **1998**, *37*, 75−78. (b) Beijer, F. H.; Sijbesma, R. P.; Kooijman, H.; Spek, A. L.; Meijer, E. W. *J. Am. Chem. Soc.* **1998**, *120*, 6761−6769. (c) Söntjens, S. H. M.; Sijbesma, R. P.; van Genderen, M. H. P.; Meijer, E. W. *J. Am. Chem. Soc.* **2002**, *122*, 7487−7493.

(13) Corbin, P. S.; Zimmerman, S. C. *J. Am. Chem. Soc.* **1998**, *120*, 9710−9711.

(14) Gong, B.; Yan, Y.; Zeng, H.; Skrzypczak-Jankunn, E.; Kim, Y. W.; Zhu, J.; Ickes, H. *J. Am. Chem. Soc.* **1999**, *121*, 5607−5608.

(15) Boileau, S.; Bouteiller, L.; Lauprêtre, F.; Lortie, F. *New J. Chem.* **2000**, *24*, 845−848.

(16) Sherrington, D. C.; Taskinen, K. A. *Chem. Soc. Rev.* **2001**, *30*, 83−93.
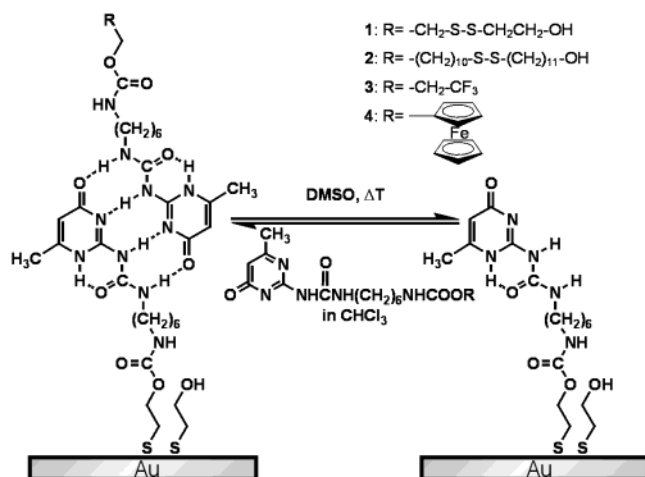
Figure 1. Complex formation of 2-ureido-4[1H]-pyrimidinone moieties at Au surfaces through quadruple hydrogen bonds can be conveniently controlled via solvent or temperature.

from 298 to 333 K].[10,12] As we show here, dithioalkyl-substituted pyrimidinones can be immobilized on gold surfaces, where they show an enhanced dependence of complex stability on the solvent composition and temperature. These features allow one to change and control the complexation behavior of substrate-immobilized pyrimidinones over a broad range, which renders this system a versatile molecular platform for the controlled immobilization or growth of complex supramolecular architectures, including supramolecular polymers.

Results and Discussion

For the study of molecular recognition on solid substrates, we have synthesized two novel asymmetrically substituted 2-ureido-4[1H]-pyrimidinone-hydroxyalkane disulfides **1** and **2**, as well as labeled external pyrimidinone guests comprising trifluoromethyl (**3**) and ferrocenyl (**4**) substitutions (Figure 1).[17] Self-assembled layers on Au were formed by spontaneous adsorption from solution and were characterized by standard techniques.[17] Depending on the choice of the solvent and, hence, K, mono- and bilayers could be formed selectively (vide infra).

Recognition between surface-immobilized adsorbates and external guests (e.g., trifluoromethyl pyrimidinone **3** in solution is recognized by pyrimidinone disulfide **1** self-assembled on Au, denoted as [Au-**1** + **3**]) occurred efficiently in CHCl$_3$, as shown by various techniques. For instance, X-ray photoelectron spectroscopy (XPS) and differential pulse voltammetry (DPV)[18] show the presence of the labeled guest molecules (Figure 2).

The recognition between SAMs of **1** on Au ([Au-**1**]) and external guests **3** and **4** in CHCl$_3$ leads to the dimeric complexes [Au-**1** + **3**] and [Au-**1** + **4**], respectively. The sequence of the XPS spectra shown in Figure 2 confirms the presence of the labels after complexation (and recomplexation upon exposure of ([Au-**1**] to **3** and **4** in CHCl$_3$), while their absence is observed after a thorough DMSO rinse, as well as for SAMs of ω-hydroxy or ω-carboxy-alkanethiols exposed to **3** or **4** under identical conditions.[17] From the ratios of the atomic percentages of F and Fe with respect to the other characteristic elements[17] determined from the corresponding F(1s) (binding energy, BE = 688.5 eV) and Fe(2p) peaks (BE = 708.5 and 723.2

eV), coverages of >45 and >50%, respectively, can be estimated.[19]

The oxidation peak of the ferrocenyl-labeled guest **4** was also detected in DPV measurements, thus confirming the molecular recognition of **4** to SAMs [Au-**1**] (Figure 2G). The peak consistently disappeared by decomplexation (Figure 2H) and reappeared after repeated recognition (Figure 2I). Hence, molecular recognition between [Au-**1**] and **3**, as well as **4**, in CHCl$_3$ proceeds efficiently. The upper limit of residual coverage of **4** after the DMSO rinse can be estimated as <4% from the XPS and DPV experiments (Figure 2).

Interestingly, dimeric complexes in layers of [Au-**1** + **n**] are stable in contact with pure CHCl$_3$ for longer than 20 h without detectable loss of the complexed guest,[17] compared to the half-life time of 170 ms of neat pyrimidinone dimers in CDCl$_3$ solution.[12c] We can conclude that surface-immobilization leads to a dramatic increase in the apparent lifetime of the dimeric 2-ureido-4[1H]-pyrimidinone complexes and, thus, significantly enhances the control of the supramolecular architecture by variations of solvent and temperature. This increase in the apparent lifetime is partially related to an altered environment (dispersion forces and solvation) of the complexes near the SAM surface and, hence, a different activated complex of the dissociation reaction involved. However, more detailed studies are needed to confirm this assertion.

In addition to directly determining the (optical) thickness of the layers and assemblies obtained, surface plasmon resonance (SPR)[6,20] measurements were applied to confirm the reversibility of the complexation. The thicknesses measured in air, assuming a refractive index of the organic layer of 1.50, are summarized in Table 1.

The data show that 2-ureido-4[1H]-pyrimidinone-hydroxyalkane disulfide **1** assembled onto Au from DMSO forms a monolayer ([Au-**1**]), while the assembly from CHCl$_3$ leads to a layer with twice the thickness. The upper leaflet of the bilayer ([Au-**1** + **1**]) can be removed by a treatment of the layer in hot CHCl$_3$;[17] it can also be washed off by DMSO, but not by CHCl$_3$, which indicates that interfacial hydrogen bonding is indeed responsible for the molecular recognition. Consequently, external pyrimidinone guests with a spectroscopic label can be assembled onto the monolayer.

Independently, we determined the thickness differences of the various architectures using contact-mode atomic force microscopy (AFM).[21] Onto a microcontact-printed matrix of octadecanethiol (ODT),[22] **1** was assembled from CHCl$_3$ in circular areas exposing bare Au. As seen in Figure 3, the height differences between the ODT matrix and the bilayer structure, as well as the different architectures obtained by rinsing with DMSO and reassembly of **1**, are in good agreement with the optical thickness determined by SPR (Table 1) and are consistent with the proposed model (Figure 1).

Thus, the combined labeling and thickness measurements confirm the scenario proposed in Figure 1. Assembly of **1** (or **2**)[23] on Au from DMSO yields monolayers, while layers formed from CHCl$_3$ resemble bilayers, that is,

(17) See Supporting Information.
(18) Kaifer, A. E.; Gomez-Kaifer, M. *Supramolecular Electrochemistry*; Wiley-VCH: Weinheim, 1999.

(19) Wagner, C. D.; Riggs, W. M.; Davis, L. E.; Moulder, J. F. In *Handbook of X-Ray Photoelectron Spectroscopy*; Muilenberg, G. E., Ed.; Perkin-Elmer Corporation: Eden Prairie, MN, 1979.
(20) Knoll, W. *Annu. Rev. Phys. Chem.* **1998**, *49*, 569–638.
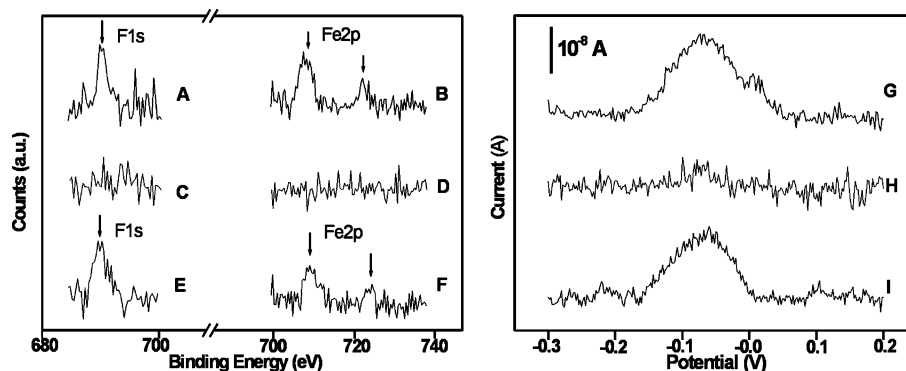(21) Magonov, S. N.; Whangbo, M.-H. *Surface Analysis with STM and AFM*; VCH: Weinheim, 1996.
(22) Xia, Y. N.; Whitesides, G. M. *Annu. Rev. Mater. Sci.* **1998**, *28*, 153–184.
(23) We did not observe pronounced differences between SAMs of **1** and **2** regarding the complexation experiments.

Figure 2. Left: high-resolution XPS spectra of (A) [Au-**1** + **3**] in CHCl$_3$ and (B) [Au-**1** + **4**] in CHCl$_3$, (C and D) after rinsing [Au-**1** + **3**] and [Au-**1** + **4**] with DMSO, and (E and F) repeated recognition of **3** and **4** by [Au-**1**] to yield [Au-**1** + **3**] and [Au-**1** + **4**], respectively. Right: DPV voltammograms (0.1 M NaClO$_4$, Hg/HgSO$_4$ reference electrode, pulse time 50 ms, interval time 200 ms, pulse height 10 mV) of (G) [Au-**1** + **4**] in CHCl$_3$, (H) after rinsing with DMSO, and (I) repeated recognition of **4** by [Au-**1**] to yield [Au-**1** + **4**].
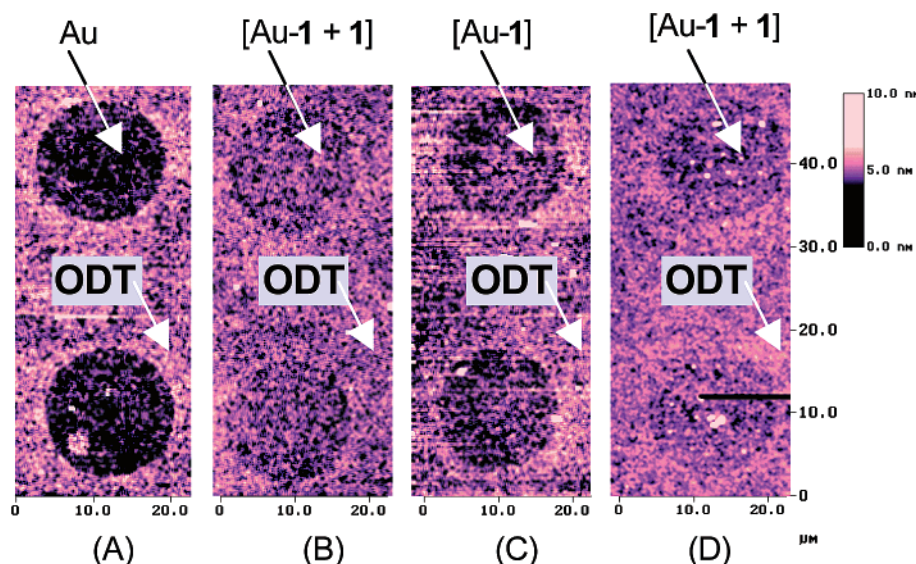
Figure 3. Contact mode AFM height images of microcontact-printed layers; outside the circles, ODT; inside the circles, (A) bare Au (ODT thickness 1.5 ± 0.3 nm), (B) [Au-**1** + **1**] (thickness 1.1 ± 0.2 nm), (C) after rinsing with DMSO [Au-**1**] (thickness 0.7 ± 0.2 nm), (D) layer after exposure to **1** in CHCl$_3$, [Au-**1** + **1**] (thickness 1.1 ± 0.3 nm). The thicknesses of the assemblies were calculated from the differences of the mean heights with respect to ODT.

Table 1. Optical Thicknesses Measured by SPR

thickness (nm) of **1** assembled on Au (solvent)	thickness (nm) of layers after DMSO rinse	thickness (nm) of [Au-**1**] treated with **3** and **4** in CHCl$_3$
0.8 ± 0.2 (DMSO)	0.7 ± 0.2	1.5 ± 0.2[a] 1.6 ± 0.2[b]
1.4 ± 0.2 (CHCl$_3$)	0.8 ± 0.2	1.6 ± 0.2[a] 1.6 ± 0.2[b]

[a] Treated with **3**. [b] Treated with **4**.

hydrogen-bonded dimeric complexes of the surface-immobilized **1** (or **2**). In case of solutions containing a disulfide adsorbate and another substituted pyrimidinone in 1:15 stoichiometry, we also observe "bilayers" of the corresponding complexes. All observations can be explained with the equilibrium concentrations of monomeric versus dimeric species in solution.[10,12]

Conclusions

SAMs of asymmetric 2-ureido-4[1H]-pyrimidinone-hydroxyalkane disulfide adsorbates on gold show efficient and controllable self-complementary molecular recognition of the pyrimidinone moieties mediated by quadruple hydrogen-bonding sites. The observed surface-enhanced

apparent dimerization constant can be tuned by solvent composition and temperature, which allows us to control the complex stability. This feature opens the possibility for the construction of more complex, directionally defined surface-immobilized supramolecular architectures, as well as for the study of pyrimidinone-based supramolecular polymers at surfaces and interfaces.

Methods

Preparation of Substrates. Sample substrates (200 nm gold on 2 nm Ti primer deposited onto glass substrates in a vacuum of 5 × 10^{-6} mbar) were purchased from SSENS bv (Hengelo, The Netherlands). Prior to use, these substrates were cleaned in piranha solution [3:1 H$_2$SO$_4$/H$_2$O$_2$ (30%) by volume], then rinsed with Milli-Q water and ethanol, and dried in a nitrogen stream. *Caution: Piranha solution should be handled with extreme caution. It has been reported to detonate unexpectedly.*

Preparation and Characterization of Monolayers. Monolayers were formed by immersing the gold substrates into a dilute solution of the corresponding compound and solvent for 10 h (typical concentration: 1 mM). After rinsing in pure solvent and drying in a N$_2$ stream, the measurements were performed with minimal delay. The layers formed were characterized by AFM, grazing incidence reflection Fourier transform infrared spectroscopy, contact angle measurements, electrochemistry, XPS, and SPR, as described previously.[24] All data confirmed the highly

reproducible formation of layers with the expected chemical composition, thickness, and order.

XPS. XPS spectra were recorded using a PHI Quantum 2000 Scanning ESCA microprobe. Spectra were acquired using a monochromated X-ray beam (Al anode), 100-μm-diameter/25-W X-ray beam scanned over a 1000 × 500 μm area at a takeoff angle of 30°. Atomic concentrations were determined by numerical integration of the relative peak areas in the detailed element scans using the following sensitivity factors: C(1s) [0.314], N(1s) [0.499], O(1s) [0.733], S(2p) [0.717], F(1s) [1.0], and Fe(2p) [2.946].

SPR Measurements. Experiments were carried out on a home-built SPR setup,[25a] which is based on the configuration introduced by Kretschmann and Raether.[25b] A refractive index of n = 1.50 was assumed for all organic adlayers.

DPV. Measurements were performed using an Autolab PGSTAT10 potentiostat (ECOCHEMIE, Utrecht, The Netherlands) in a three-electrode configuration. The gold sample covered with the corresponding layer was used as the working electrode, Hg/HgSO$_4$ (MSE) was used as the reference (+0.61 V$_{NHE}$), and a Pt wire was used as the auxiliary electrode. The electrolyte was 0.1 M NaClO$_4$. The working electrode exposed a surface area of 0.44 cm^2 to the electrolyte. Prior to the measurements,

the cell was degassed by passing nitrogen through the electrolyte for 5 min. DPV voltammograms were recorded at a pulse amplitude of 10 mV, a pulse time of 50 ms, and a time interval of 200 ms.

AFM Measurements. The measurements were carried out with a NanoScope III AFM microscope (Digital Instruments, Santa Barbara, CA) in the contact mode. Constant-force AFM scans were performed in air with a load of 3 nN using V-shaped Si$_3$N$_4$ cantilevers [Nanoprobes (DI), spring constant of 0.1 N/m]. The calibration of the AFM scanner in the z direction was carried out using a set of three vertical calibration standards (TGZ 01-03) with step heights of 25.5, 104, and 512 nm, respectively (Silicon-MDT, Moscow, Russia). All the images shown here were subjected to a first-order plane-fitting procedure to compensate for sample tilt and to a zeroth-order flattening.

Supporting Information Available: Additional data (XPS, DPV, and SPR) and chemical syntheses. This material is available free of charge via the Internet at http://pubs.acs.org.

LA030127C

(24) (a) Schönherr, H.; Ringsdorf, H. *Langmuir* **1996**, *12*, 3891−3897. (b) Schönherr, H.; Vancso, G. J.; Huisman, B.-H.; van Veggel, F. C. J. M.; Reinhoudt, D. N. *Langmuir* **1997**, *13,* 1567−1570. (c) Peter, M.; Hempenius, M. A.; Lammertink, R. G. H.; Vancso, G. J. *Macromol. Symp.* **2001**, *167*, 285−296.

(25) (a) Rothenhäusler, B.; Knoll, W. *Nature* **1988**, *332*, 615−617. (b) Kretschmann, E.; Raether, H. *Z. Naturforsch.* **1968**, *23A*, 2135−2136.